



HAL
open science

Miniature multimodal endoscopic probe based on double-clad fiber

Xianjin Dai, Haomiao Yang, Jianbo Tang, Can Duan, Quentin Tanguy, Huikai Xie, H Jiang

► **To cite this version:**

Xianjin Dai, Haomiao Yang, Jianbo Tang, Can Duan, Quentin Tanguy, et al.. Miniature multimodal endoscopic probe based on double-clad fiber. SPIE BIOS - Endoscopic Microscopy, Jan 2017, San Fransisco, United States. 10.1117/12.2251510 . hal-03053080

HAL Id: hal-03053080

<https://hal.science/hal-03053080>

Submitted on 18 May 2022

HAL is a multi-disciplinary open access archive for the deposit and dissemination of scientific research documents, whether they are published or not. The documents may come from teaching and research institutions in France or abroad, or from public or private research centers.

L'archive ouverte pluridisciplinaire **HAL**, est destinée au dépôt et à la diffusion de documents scientifiques de niveau recherche, publiés ou non, émanant des établissements d'enseignement et de recherche français ou étrangers, des laboratoires publics ou privés.



Distributed under a Creative Commons Attribution - NonCommercial 4.0 International License

Miniature multimodal endoscopic probe based on double-clad fiber

Xianjin Dai^a, Hao Yang^a, Jianbo Tang^a, Can Duan^b, Quentin Tanguy^b, Huikai Xie^b, and Huabei Jiang^{a,*}

^aJ. Crayton Pruitt Family Department of Biomedical Engineering, University of Florida, Gainesville, Florida 32611, United States;

^bDepartment of Electrical and Computer Engineering, University of Florida, Gainesville, Florida 32611, United States

ABSTRACT

Optical coherence tomography (OCT) can obtain light scattering properties with a high resolution, while photoacoustic imaging (PAI) is ideal for mapping optical absorbers in biological tissues, and ultrasound (US) could penetrate deeply into tissues and provide elastically structural information. It is attractive and challenging to integrate these three imaging modalities into a miniature probe, through which, both optical absorption and scattering information of tissues as well as deep-tissue structure can be obtained. Here, we present a novel side-view probe integrating PAI, OCT and US imaging based on double-clad fiber which is used as a common optical path for PAI (light delivery) and OCT (light delivery/detection), and a 40 MHz unfocused ultrasound transducer for PAI (photoacoustic detection) and US (ultrasound transmission/receiving) with an overall diameter of 1.0 mm. Experiments were conducted to demonstrate the capabilities of the integrated multimodal imaging probe, which is suitable for endoscopic imaging and intravascular imaging.

Keywords: Optical coherence tomography, photoacoustic imaging, ultrasound, multimodal imaging, endoscopy

1. INTRODUCTION

Photoacoustic imaging (PAI) Multimodal imaging is always attractive and desired since it can combine the strengths of several different imaging modalities, and is able to characterize biological tissue more completely, thus offering the possibility of precision diagnosis of diseases. While multimodality images can be obtained by performing each individual modality separately without integrating them into a single platform, it is, however, time-consuming to acquire multimodality images through such a process, hard to avoid errors from the required complex image registration, and more importantly, impossible to catch dynamic biological processes simultaneously. To overcome these limitations, physically integrating multiple modalities into a single platform is highly desired. Among recent advances in biomedical imaging, photoacoustic imaging (PAI) is an emerging technique capable of providing anatomical, functional, molecular properties of biological tissue with a high resolution [1-9]. In PAI, an image is formed through the detection of laser-induced ultrasound waves with an (un)focused ultrasound transducer. Since ultrasound (US) can penetrate into deep tissue, and a common ultrasound transducer can be used for both US and PAI, these two modalities have been combined as a dual-modality approach for obtaining both images of optical absorption property and deep tissue structure [10-18].

Optical coherence tomography (OCT) is a widespread imaging technique by measuring back-scattered or back-reflected light generated from a light source delivered to the examined tissue, which is able to provide optical scattering property of tissue in high resolution [19, 20]. While OCT is ideal for imaging retina [21-23], it has also been used to visualize other tissues [24-27]. Thus, through combining PAI and OCT, both optical absorption and back-scattering information can be obtained. In this regard, we and other groups have made efforts to develop an integrated platform combining PAI and OCT [28-34]. These studies have demonstrated the advantages of such a dual-modality system. For example, for in vivo microcirculation studies, PAI provided absorbing components such as blood vessels, while OCT obtained the fine structures of the surrounding tissues.

* hjjiang@bme.ufl.edu; phone 1 (352) 273-9336; fax 1 (352) 273-9221.

It is conceivable that a multimodal approach integrating PAI, OCT and US would provide a more powerful tool for tissue imaging. In this regard, we and other groups took initial steps towards the integration of such three modalities in a single probe. The study of Yang et al. [35], while inspiring, PAI, OCT and US were not physically integrated in a single probe with a diameter of 5 mm for imaging ovarian tissue, and PAI in their probe could not visualize microvasculature due to its relatively poor spatial resolution.

We [36] demonstrated a miniature tri-modal probe with a diameter of 2 mm, physically integrating OCT, US, and optical-resolution photoacoustic microscopy (OR-PAM) (which is one of PAI modes). The use of a gold-coated thin film in this probe allowed us, for the first time, to coaxially acquire OR-PAM, OCT and US images of the same area of biological tissue *in vivo*. While encouraging, this 2mm-diameter tri-modal probe cannot be used for clinical intravascular and transurethral imaging or for preclinical studies of internal organs in small animals. For example, internal organs such as colon of nude mouse is so small in size that a 2mm-diameter probe would simply break the colon. [37] Although the urethra of an adult is about 5-7 mm in diameter for men and larger for women, the ureteral wall injury happens very often while ureteroscopy is performed. [38] In particular, a critical size of 1 mm or smaller is required for clinical intravascular imaging. It is, however, rather challenging to engineer a tiny multimodal probe having a diameter of 1 mm or smaller. In the following sections, we describe how we tackled the challenges to develop a novel probe integrating PAI, OCT, and US with a diameter of only 1.0 mm based on a double-clad fiber (DCF).

2. MATERIAL AND METHODS

2.1 Multimodal imaging probe

The structure of the probe is schematically shown in Fig. 1. In this probe, a DCF with a dual cladding structure (DCF13, Thorlabs), in which, single-mode light travels in the $\varnothing 9 \mu\text{m}$ core with a numerical aperture (NA) of 0.12 and a spectrum range of 1250 – 1600 nm, while multi-mode light propagates in the $\varnothing 105 \mu\text{m}$ inner first cladding (NA = 0.2, 400 – 2200 nm), is used to deliver light for both PAI (multi-mode) and OCT (single-mode). A custom-designed gradient-index (GRIN) lens with a diameter of 0.25 mm and a working distance of 5 mm (GRINTECH GmbH) is utilized to focus the light beam including single-mode (indicated by red dotted line) and multi-mode (indicated by green area) from the tip of DCF with 8° angle facial cutting for minimizing back-reflection. Travelling through a piece of 45° -angle-tilting reflection slide (which is optically transparent but ultrasonically untransparent), the light beam is then reflected into the sample by a 0.5-mm enhanced-aluminum-coated right-angle prism (MPCH-0.5, Tower Optical Corp.). For OCT, the back-scattering light from sample shares the same optical path with light transmission. For PAI, the light-induced photoacoustic signals reflected by prism and reflection slide, are detected by a custom-made unfocused ultrasound transducer with a center frequency of 40 MHz and a dimension of $0.6 \text{ mm} \times 0.5 \text{ mm} \times 0.2 \text{ mm}$ (Blatek, Inc., State College, PA) mounted coaxially with respect to the optical path. The transducer is also used for US imaging, in which, an image is formed by detecting the echo of the pulsed ultrasound generated by the same transducer. All the components are fixed by three stainless steel tubes (260 μm , 500 μm , and 1000 μm in diameter).

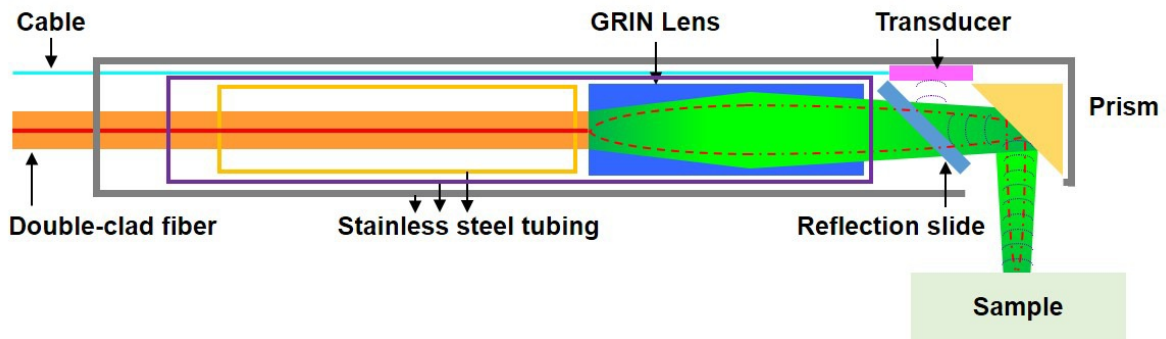


Figure 1. Schematic of the integrated multimodal probe.

2.2 Multimodal imaging system

The integrated multimodal imaging system is schematically shown in Fig. 2. For PAI, a nanosecond pulsed Nd:YAG pumped Optical Parametric Oscillator (OPO) laser having a repetition frequency of 20 Hz was used as light source. The light beam attenuated by a neutral density (ND) filter, and then shaped by a small iris, was focused by a convex lens

(L1); the light beam then passed through a 100- μm pinhole for spatial filtering and was coupled into a multimode fiber (MMF) (FG105LCA, Thorlabs). Since a time-domain OCT system was available in our laboratory, hereafter, it was used to demonstrate the feasibility of the integrated probe (this OCT system is compatible to any state-of-art OCT system such as swept source OCT). A broadband light source with a full width at half-maximum (FWHM) of 75 nm and a center wavelength of 1310 nm was utilized for the time-domain OCT system, the optical interface of which was a single mode fiber (SMF) (SMF-28e+, Thorlabs). Through a home-made DCF coupler, consisting of four convex lenses and a short-pass dichroic mirror (DM) (DMSP1180, Thorlabs), the integrated probe was coupled with both PAI and OCT systems based on DCF. A data acquisition (DAQ) card (PCI-5124, National Instrument) embedded in a computer (PC) with 12-bit resolution and a sampling rate of 200 MS/s was utilized as the data acquisition system. For US imaging, an ultrasound pulser/receiver (5073PR, Olympus) with an integrated amplifier and a bandwidth of 75 MHz was utilized to generate ultrasound and to receive echoes. By scanning the probe in x-y plane with a two-dimensional (2D) linear stage, a volumetric image of the sample could be obtained.

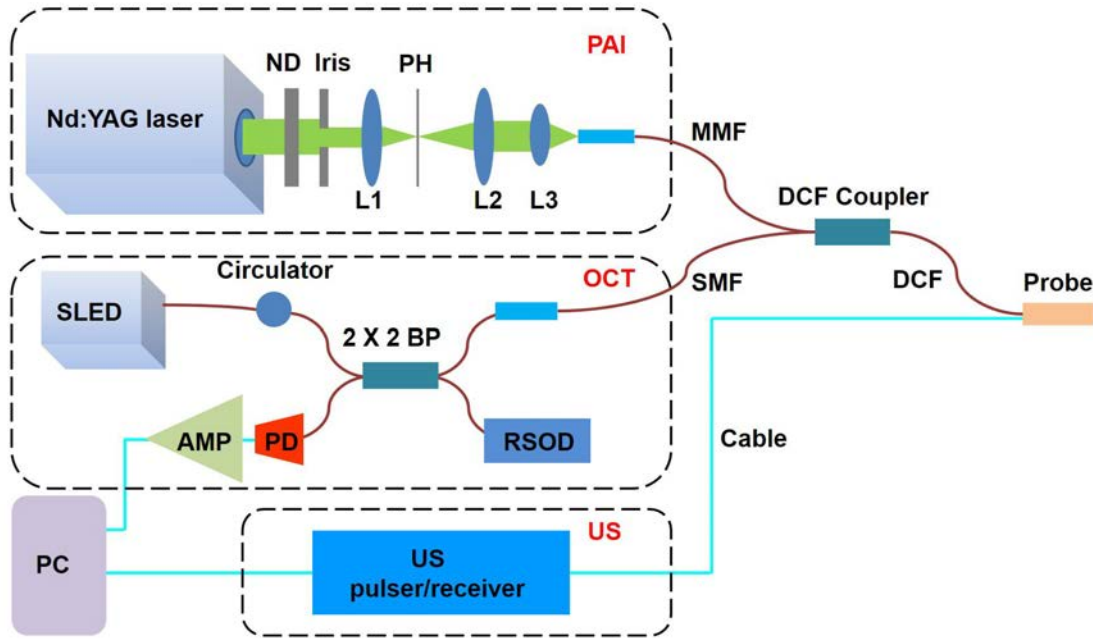


Figure 2. Integrated multimodal imaging system. ND, neutral density filter; L1, L2, L3, lenses; PH, pinhole; BP, beam splitter; PD, photodiode, AMP, amplifier; RSOD, rapid scanning optical delay; PC, personal computer; MMF, multimode fiber; SMF, single mode fiber; DCF, double-clad fiber.

3. RESULTS AND DISCUSSION

3.1 *In vivo* imaging of a mouse ear

In vivo imaging of a mouse ear (mouse weight=35g) was firstly performed to demonstrate the capabilities of this integrated multimodal probe. The laser exposure was about 10 mJ/cm^2 at the optical focus inside the ear tissue which is lower than the American National Standards Institute (ANSI) laser safety limit (20 mJ/cm^2). An area of $2 \text{ mm} \times 2 \text{ mm}$ of the mouse ear was scanned with a scanning step size of $10 \mu\text{m}$, which took around 36 minutes.

The top row of Fig. 3 shows the maximum amplitude projection (MAP) images of PAI (Fig. 3(a)), US (Fig. 3(b)), OCT (Fig. 3(c)), and fused multimodal pseudo-color-coded RGB images (Fig. 3(d)) obtained from PAI (R, red), OCT (G, green), US (B, blue). The middle and bottom rows of Fig. 3 show the cross-sectional images of PAI, US, OCT, and fused multi-modality, corresponding to the two dotted lines in the respective MAP images. We see that PAI, OCT and US, respectively, were able to image the microvasculature, fine structures surrounding the blood vessels and elastic structures. To closely interpret these images, blood vessels in the mouse ear are mapped by PAI with the highest contrast

(Fig. 3(a)), elastic structures like cartilage, which have high ultrasound reflection coefficients are clearly visualized by US (Fig. 3(b)), while epidermis, dermis, and cartilage are identified in OCT image (Fig. 3(c)). Through overlapping the PAI, OCT, and US images (Fig. 3(d)), the structures/tissue morphology are better displayed, which shows in vivo imaging feasibilities of the integrated multimodal probe.

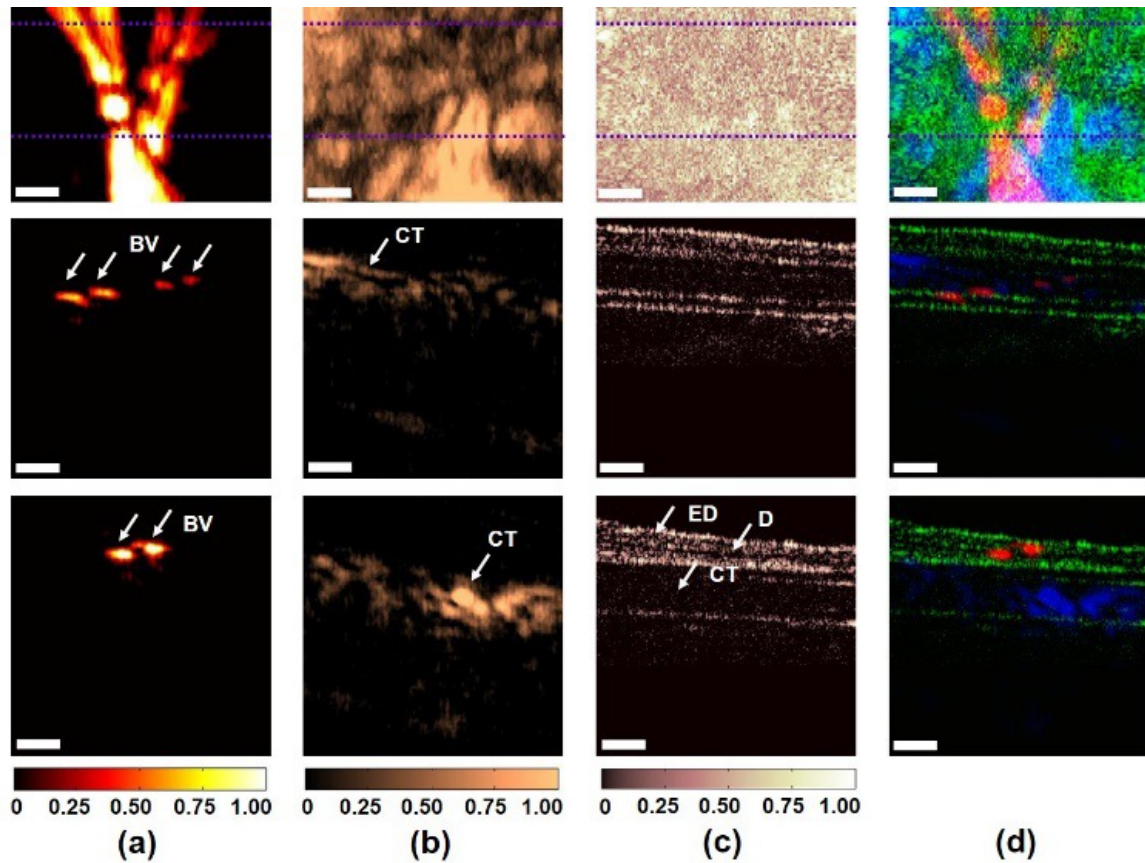


Figure 3. In vivo images of a mouse ear. Maximum amplitude projection (MAP) (top row) and cross-sectional images (middle and bottom rows) corresponding to the dotted lines shown in the MAP image of (a) PAI, (b) US, (c) OCT, and (d) Fused tri-modality. BV, blood vessel; ED, epidermis; D, dermis; CT, cartilage. The scale bars indicate 0.3 mm in length.

3.2 In vivo imaging of human hand

We then conducted in vivo imaging of the back of a human hand to explore the potential clinical capabilities of the integrated multimodal probe. A step size of 10 μm was used for scanning the back of hand, and it took around 15 seconds to obtain a b-scan (cross-sectional) image. Figs. 4(a), 4(b) and 4(c), respectively, show the cross-sectional images of the hand from PAI, US and OCT. Using the same RGB pseudo-coding method as the one used for mouse ear imaging, the fused multimodal image is given in Fig. 4(d). Fig. 4(e) is the photograph of the scanning location on the surface of hand indicated by red dotted line.

From Fig. 4, it is noted that blood vessels (as indicated by a white arrow in Fig. 4(a)), superficial fine structures and elastic structures (such as bone, as indicated by a white arrow in Fig. 4(b)) are identified by PAI, OCT and US, respectively. Since typically the thickness of mouse ear is less than 2 mm, the deep penetration ability of US was not demonstrated from images shown in Fig. 3(b). Here, in Fig. 4(b), it is evident that US can image the structure of tissue up to 5 mm in depth. Carefully examining Figs. 4(b) and 4(c), we note that superficial surface of tissue having less ultrasonic reflection can be complementarily visualized by OCT with a high resolution. From the fused image (Fig. 4(d)), we can see that the morphology of tissue with a depth of up to 5 mm was mapped by our integrated probe with a high resolution and that different tissues were imaged by the three different imaging modalities.

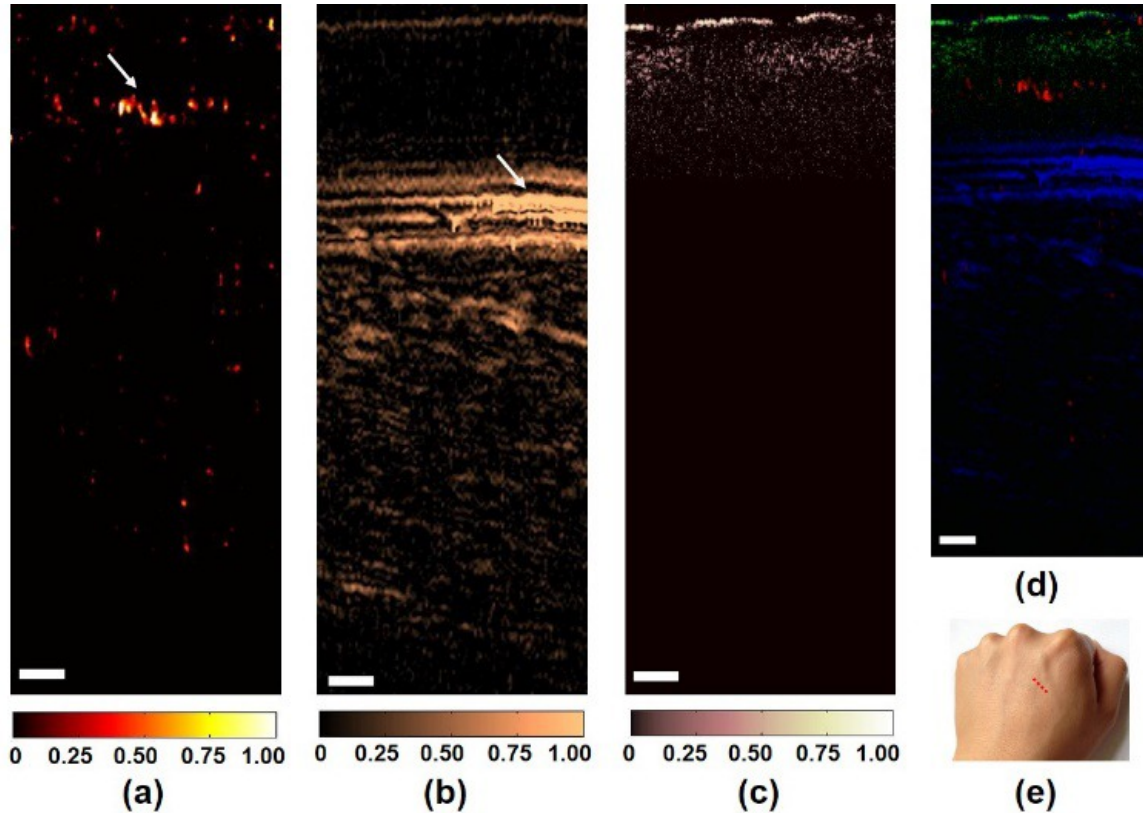


Figure 4. Cross-sectional images of the skin of human hand. (a) PAI image, (b) US image, (c) OCT image, (d) Color-coded RGB image, and (e) Photograph of the scanning location. The scale bars indicate 0.3 mm in length.

4. CONCLUSION

In summary, we have developed a novel miniature device of only 1.0 mm in diameter that integrated PAI, OCT and US in a single probe based on a double-clad fiber. The results from in vivo experiments have shown that the integrated multimodal probe has the capability of simultaneously obtaining optical absorption and scattering properties of biological tissue as well as tissue elastic characters in high resolution. We have further exploited the abilities of the integrated multimodal probe for multimodal endoscopic imaging[39]. We noted that in our experimental setup, the imaging speed was limited by a relatively low repetition frequency of nanosecond pulsed Nd:YAG pumped OPO laser (20 Hz), and a relatively slow approach of time-domain OCT. Nevertheless, the advanced probe presented here can be adapted easily with any high-speed PAI system and state-of-art OCT imaging system (such as high-speed swept source OCT). The highly integrating and miniature size of the probe has the potential to generate significant impact in preclinical and clinical applications such as multimodal intravascular coronary imaging, in vivo imaging of internal organs in small animals, ureteroscopy/transurethral imaging, and minimally invasive interventional therapy.

5. ACKNOWLEDGEMENTS

We acknowledge the generous financial support from the J. Crayton Pruitt Family Endowment.

REFERENCES

- [1] V. Ntziachristos, and D. Razansky, "Molecular imaging by means of multispectral optoacoustic tomography (MSOT)," *Chemical reviews*, 110(5), 2783-2794 (2010).
- [2] L. Xiang, B. Wang, L. Ji *et al.*, "4-D photoacoustic tomography," *Scientific reports*, 3, 1113 (2013).
- [3] L. Nie, and X. Chen, "Structural and functional photoacoustic molecular tomography aided by emerging contrast agents," *Chemical Society Reviews*, 43(20), 7132-7170 (2014).
- [4] L. Xiang, M. Ahmad, X. Hu *et al.*, "Label-free photoacoustic cell-tracking in real-time," *X Acoust. Imaging Sens*, 1, 18-22 (2014).
- [5] H. Qin, T. Zhou, S. Yang *et al.*, "Fluorescence Quenching Nanoprobes Dedicated to In Vivo Photoacoustic Imaging and High Efficient Tumor Therapy in Deep Seated Tissue," *Small*, 11(22), 2675-2686 (2015).
- [6] Y. Liu, H. Jiang, and Z. Yuan, "Two schemes for quantitative photoacoustic tomography based on Monte Carlo simulation," *Medical Physics*, 43(7), 3987-3997 (2016).
- [7] J. Tang, X. Dai, and H. Jiang, "Wearable scanning photoacoustic brain imaging in behaving rats," *Journal of biophotonics*, (2016).
- [8] J. Tang, J. E. Coleman, X. Dai *et al.*, "Wearable 3-D Photoacoustic Tomography for Functional Brain Imaging in Behaving Rats," *Scientific reports*, 6, (2016).
- [9] H. Yang, L. Xi, S. Samuelson *et al.*, "Handheld miniature probe integrating diffuse optical tomography with photoacoustic imaging through a MEMS scanning mirror," *Biomedical optics express*, 4(3), 427-432 (2013).
- [10] X. Bai, X. Gong, W. Hau *et al.*, "Intravascular optical-resolution photoacoustic tomography with a 1.1 mm diameter catheter," *PloS one*, 9(3), e92463 (2014).
- [11] M. Gerling, Y. Zhao, S. Nania *et al.*, "Real-time assessment of tissue hypoxia in vivo with combined photoacoustics and high-frequency ultrasound," *Theranostics*, 4(6), 604 (2014).
- [12] P. Subochev, A. Orlova, M. Shirmanova *et al.*, "Simultaneous photoacoustic and optically mediated ultrasound microscopy: an in vivo study," *Biomedical Optics Express*, 6(2), 631-638 (2015).
- [13] Y. Cao, J. Hui, A. Kole *et al.*, "High-sensitivity intravascular photoacoustic imaging of lipid-laden plaque with a collinear catheter design," *Scientific reports*, 6, (2016).
- [14] T. Harrison, J. C. Ranasinghesagara, H. Lu *et al.*, "Combined photoacoustic and ultrasound biomicroscopy," *Optics Express*, 17(24), 22041-22046 (2009).
- [15] K. Daoudi, P. Van den Berg, O. Rabot *et al.*, "Handheld probe integrating laser diode and ultrasound transducer array for ultrasound/photoacoustic dual modality imaging," *Optics express*, 22(21), 26365-26374 (2014).
- [16] A. Garcia-Urbe, T. N. Erpelding, A. Krumholz *et al.*, "Dual-modality photoacoustic and ultrasound imaging system for noninvasive sentinel lymph node detection in patients with breast cancer," *Scientific reports*, 5, (2015).
- [17] C.-W. Wei, T.-M. Nguyen, J. Xia *et al.*, "Real-time integrated photoacoustic and ultrasound (PAUS) imaging system to guide interventional procedures: ex vivo study," *IEEE transactions on ultrasonics, ferroelectrics, and frequency control*, 62(2), 319-328 (2015).
- [18] F. Raes, J. Sobilo, M. Le Mée *et al.*, "High Resolution Ultrasound and Photoacoustic Imaging of Orthotopic Lung Cancer in Mice: New Perspectives for Onco-Pharmacology," *PloS one*, 11(4), e0153532 (2016).
- [19] D. Huang, E. A. Swanson, C. P. Lin *et al.*, "Optical coherence tomography," *Science (New York, NY)*, 254(5035), 1178 (1991).
- [20] J. G. Fujimoto, C. Pitris, S. A. Boppart *et al.*, "Optical coherence tomography: an emerging technology for biomedical imaging and optical biopsy," *Neoplasia*, 2(1), 9-25 (2000).
- [21] M. R. Hee, J. A. Izatt, E. A. Swanson *et al.*, "Optical coherence tomography of the human retina," *Archives of ophthalmology*, 113(3), 325-332 (1995).
- [22] B. White, M. Pierce, N. Nassif *et al.*, "In vivo dynamic human retinal blood flow imaging using ultra-high-speed spectral domain optical coherence tomography," *Optics express*, 11(25), 3490-3497 (2003).
- [23] W. Drexler, and J. G. Fujimoto, "State-of-the-art retinal optical coherence tomography," *Progress in retinal and eye research*, 27(1), 45-88 (2008).
- [24] B. Bouma, G. Tearney, H. Yabushita *et al.*, "Evaluation of intracoronary stenting by intravascular optical coherence tomography," *Heart*, 89(3), 317-320 (2003).
- [25] T.-H. Tsai, J. G. Fujimoto, and H. Mashimo, "Endoscopic optical coherence tomography for clinical gastroenterology," *Diagnostics*, 4(2), 57-93 (2014).
- [26] S. P. Chong, C. W. Merkle, D. F. Cooke *et al.*, "Noninvasive, in vivo imaging of subcortical mouse brain regions with 1.7 μm optical coherence tomography," *Optics letters*, 40(21), 4911-4914 (2015).

- [27] E. Jorge, R. Baptista, J. Calisto *et al.*, “Optical coherence tomography of the pulmonary arteries: A systematic review,” *Journal of cardiology*, 67(1), 6-14 (2016).
- [28] L. Li, K. Maslov, G. Ku *et al.*, “Three-dimensional combined photoacoustic and optical coherence microscopy for in vivo microcirculation studies,” *Optics express*, 17(19), 16450-16455 (2009).
- [29] X. Zhang, H. F. Zhang, and S. Jiao, “Optical coherence photoacoustic microscopy: accomplishing optical coherence tomography and photoacoustic microscopy with a single light source,” *Journal of biomedical optics*, 17(3), 0305021-0305023 (2012).
- [30] L. Xi, C. Duan, H. Xie *et al.*, “Miniature probe combining optical-resolution photoacoustic microscopy and optical coherence tomography for in vivomicrocirculation study,” *Applied optics*, 52(9), 1928-1931 (2013).
- [31] E. Z. Zhang, B. Povazay, J. Laufer *et al.*, “Multimodal photoacoustic and optical coherence tomography scanner using an all optical detection scheme for 3D morphological skin imaging,” *Biomedical optics express*, 2(8), 2202-2215 (2011).
- [32] T. Berer, E. Leiss-Holzinger, A. Hochreiner *et al.*, “Multimodal noncontact photoacoustic and optical coherence tomography imaging using wavelength-division multiplexing,” *Journal of biomedical optics*, 20(4), 046013-046013 (2015).
- [33] X. Liu, T. Liu, R. Wen *et al.*, “Optical coherence photoacoustic microscopy for in vivo multimodal retinal imaging,” *Optics letters*, 40(7), 1370-1373 (2015).
- [34] B. Zabihian, J. Weingast, M. Liu *et al.*, “In vivo dual-modality photoacoustic and optical coherence tomography imaging of human dermatological pathologies,” *Biomedical optics express*, 6(9), 3163-3178 (2015).
- [35] Y. Yang, X. Li, T. Wang *et al.*, “Integrated optical coherence tomography, ultrasound and photoacoustic imaging for ovarian tissue characterization,” *Biomedical optics express*, 2(9), 2551-2561 (2011).
- [36] X. Dai, L. Xi, C. Duan *et al.*, “Miniature probe integrating optical-resolution photoacoustic microscopy, optical coherence tomography, and ultrasound imaging: proof-of-concept,” *Optics letters*, 40(12), 2921-2924 (2015).
- [37] C. Becker, M. Fantini, S. Wirtz *et al.*, “In vivo imaging of colitis and colon cancer development in mice using high resolution chromoendoscopy,” *Gut*, 54(7), 950-954 (2005).
- [38] O. Traxer, and A. Thomas, “Prospective evaluation and classification of ureteral wall injuries resulting from insertion of a ureteral access sheath during retrograde intrarenal surgery,” *The Journal of urology*, 189(2), 580-584 (2013).
- [39] X. Dai, H. Yang, T. Shan *et al.*, “Miniature Endoscope for Multimodal Imaging,” *ACS Photonics*, (2016).